



Reduction of Permeability in Granite at Elevated Temperatures

Author(s): Diane E. Moore, David A. Lockner and James D. Byerlee

Source: *Science*, New Series, Vol. 265, No. 5178 (Sep. 9, 1994), pp. 1558-1561

Published by: [American Association for the Advancement of Science](#)

Stable URL: <http://www.jstor.org/stable/2884559>

Accessed: 27/05/2014 17:45

Your use of the JSTOR archive indicates your acceptance of the Terms & Conditions of Use, available at <http://www.jstor.org/page/info/about/policies/terms.jsp>

JSTOR is a not-for-profit service that helps scholars, researchers, and students discover, use, and build upon a wide range of content in a trusted digital archive. We use information technology and tools to increase productivity and facilitate new forms of scholarship. For more information about JSTOR, please contact support@jstor.org.



American Association for the Advancement of Science is collaborating with JSTOR to digitize, preserve and extend access to *Science*.

<http://www.jstor.org>

Reduction of Permeability in Granite at Elevated Temperatures

Diane E. Moore,* David A. Lockner, James D. Byerlee

The addition of hydrothermal fluids to heated, intact granite leads to permeability reductions in the temperature range of 300° to 500°C, with the rate of change generally increasing with increasing temperature. The addition of gouge enhances the rate of permeability reduction because of the greater reactivity of the fine material. Flow rate is initially high in a throughgoing fracture but eventually drops to the level of intact granite. These results support the fault-valve model for the development of mesothermal ore deposits, in which seals are formed at the base of the seismogenic zone of high-angle thrust faults. The lower temperature results yield varying estimates of mineral-sealing rates at shallower depths in fault zones, although they generally support the hypothesis that such seals develop in less time than the recurrence interval for moderate to large earthquakes on the San Andreas fault.

Studies of active and exhumed faults have demonstrated the importance of fluids and fluid-rock interactions to fault-zone processes at depth (1–3). Mineral-sealing processes, in particular, may be significant in explaining the evolution of fluid pressures in fault zones, and some recent models of the earthquake cycle invoke the development of mineral seals within faults in the intervals between earthquakes (3, 4). Successful testing and application of these models requires knowledge of the evolution of permeability over time for rock and gouge materials at elevated temperatures and pressures. To this end, we measured the permeability of Westerly granite under hydrothermal conditions, in experiments up to 6 weeks in length. The principal minerals of Westerly granite—plagioclase, quartz, and K-feldspar—are the most commonly occurring minerals in the Earth's crust, and their response to hydrothermal conditions is applicable to a wide range of rock types involved in continental faulting.

In the main series of experiments, cylinders of granite 21.9 mm long and 19.1 mm in diameter were placed between insulating pieces of aluminum oxide in a copper jacket. The jacketed sample fit inside a cylindrical furnace in a triaxial deformation apparatus (5). The fluid pressure at the ends of the granite cylinder was maintained constant by two pumps. During an experiment, these pumps were set to maintain the pore pressure on one side of the sample at 2.0 MPa above the pressure on the other side to produce steady-state flow through the sample. The high and low pore-pressure sides of the sample were reversed periodically during each experiment to measure permeability in both directions and to keep the same

fluid in contact with the sample (6).

We investigated crack healing and sealing rates and associated permeability changes as a function of temperature (7); parameters such as confining and fluid pressure, differential stress, rock-to-water ratio, and especially fluid chemistry will be varied in future experiments. The experiments here were run at temperatures between 300° and 500°C (Table 1), with confining and pore pressures kept constant at 150 MPa and 100 MPa, respectively. Duplicate experiments showed excellent repeatability of the results. Deionized water was the starting pore fluid (6). Most of the experiments were conducted on intact cylinders of Westerly granite, but we also tested two configurations at 400°C that are of significance to fault zones. One configuration consists of a layer of granite gouge (8) sandwiched between granite end pieces used to determine the effect of fault gouge on the rate of permeability change. The other sample was fractured in tension parallel to the axis of the cylinder, simulating the fractured country rock adjacent to a fault zone.

For the intact and sandwich samples, we determined permeability, k (in square meters), by measuring the flow rate at intervals over the constant pore-pressure drop of 2.0 MPa, assuming that Darcy's law holds (9). In the case of the fractured sample, resistance to flow was calculated in terms of the parameter λ (in cubic meters) (9). The room-temperature permeability of intact Westerly granite at an effective pressure of 50 MPa is in the range of 5×10^{-20} to 1×10^{-19} m² (10). The initial heated permeability values (Table 1) in our experiments were higher than this room-temperature range because of thermal cracking accompanying heating (11). The amount of increase among the intact samples varied roughly linearly with temperature (Table 1), consistent with the changes in permeability predicted from the physical properties of Westerly granite at elevated temperatures and pressures (12). Permeability decreased over time in all experiments. For most of the intact-rock experiments (Fig. 1), the rate of decrease was rapid for the first 1 to 2 days after heating but subsequently dropped to a uniform rate that in most cases continued until the end of the experiment. In contrast, both of the experiments at 500°C (Fig. 1D) were characterized by a rapid decrease in k after 5 to 6 days. The final permeability measurement of 500i-2 was roughly three orders of magnitude below the initial heated value, and flow through the sample had in effect ceased. Experiment 500i-1 differed somewhat in that, after decreasing to 2×10^{-21} m², the permeability partly recovered to 3×10^{-20} m². The cause of the rapid decline in k at 500°C has not yet been determined.

Overall, the rate of permeability reduction increased with increasing temperature in the examined range, but with some reversals. For example, k decreased somewhat more rapidly at 400°C than at 450°C, as indicated by the different slopes (Fig. 1C). The data from both experiments at 300°C also have steeper slopes than the nearly flat

Table 1. Summary of intact-rock and sandwich experiments, conducted at 150 MPa confining pressure, 100 MPa pore pressure, and 2.0 MPa differential pore pressure across the sample. All samples were intact, except for 400s, which was sandwich.

Experiment	Duration (days)	T (°C)	k (initial) (10^{-21} m ²)	k (final) (10^{-21} m ²)	$r \pm 2\sigma$ ($\times 10^{-9}$) in $k = c(10^{-r})$
300i-1	19.5	300	166.1	59.1	8.10 ± 0.70
300i-2	17.6	300	99.6	56.5	8.30 ± 1.02
350i-1	13.6	350	171.5	92.0	3.41 ± 1.21
350i-2	19.1	350	170.0	91.5	0.80 ± 0.82
400i	45.8	400	137.6	18.3	19.08 ± 0.56
400s	23.7	400	1230.9	171.8	—
450i-1	19.8	450	364.5	129.9	13.49 ± 0.33
450i-2	20.0	450	404.0	121.4	14.50 ± 0.35
500i-1	11.0	500	326.8	19.4	65.25 ± 16.95
500i-2	9.8	500	465.4	0.4 ± 0.4	41.25 ± 3.93

U.S. Geological Survey, Mail Stop 977, 345 Middlefield Road, Menlo Park, CA 94025, USA.

*To whom correspondence should be addressed.

trends of the two experiments at 350°C (Fig. 1, A and B). A similar reversal in the rate of permeability decrease has been observed for granular aggregates of quartz and plagioclase (13).

To quantify the rates of permeability change, an exponential equation of the form

$$k = c(10^{-rt}) \quad (1)$$

was fit by least-square methods to the uniform part of each intact rock experiment in Fig. 1 (14). For consistency, the data from the first 2.0 days of each experiment were excluded from the calculations. The rapidly decreasing permeability values at the ends of experiments 500i-1 and 500i-2 also were omitted. The calculated values of r (± 2 SD) are listed in Table 1 and plotted relative to the temperature of each experiment in Fig. 2. The figure clearly displays the varying rates of permeability change suggested by the data in Fig. 1. The very low slopes of the data from the 350°C experiments (Fig. 1B) lead to the large relative error estimates for those determinations of r .

Because of its large initial k (Table 1), the permeability of sandwich sample 400s remained higher than that of intact sample 400i throughout the experiments (Fig. 3A). The overall rate of permeability change

during experiment 400s also differed from those of the other intact rock experiments. For the first 10 to 12 days, permeability decreased more rapidly in the gouge-bearing sample than in the intact sample, although the final rates of permeability decrease for experiments 400s and 400i were similar.

Flow through the fractured sample 400f was initially rapid, and for the first few days only a small pore-pressure gradient could be maintained across the sample at the maximum flow rate of the pump (Table 2). Values of λ were fairly constant for the first 10 days of the experiment (Fig. 3B). Subsequently, however, the differential pore pressure first increased to the 2.0-MPa set point, and then the flow rates measured over the 2.0-MPa pore-pressure drop began to decrease rapidly. By day 17, λ had decreased nearly three orders of magnitude, such that the rate of fluid flow was at the level of the intact sample 400i. In Table 2, the final permeability measurement is calculated in terms of k as well as λ ; the value of k is consistent with the 3.2×10^{-20} to 3.8×10^{-20} m² range of k obtained during day 28 of experiment 400i (Fig. 3A).

Petrographic investigation of the causes of permeability change is currently underway (6). However, the fractured sample (400f) is briefly described here as an illustration of the processes leading to the permeability reductions. Scanning electron mi-

croscope (SEM) examination of the separated fracture surfaces revealed widespread evidence of mineral dissolution and precipitation (Fig. 4). The feldspar and especially the quartz surfaces were rounded by dissolution, and some quartz and K-feldspar crys-

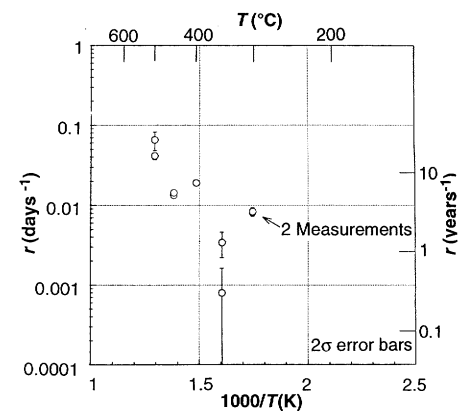


Fig. 2. Plot of the coefficient r of exponential equations of the form $k = c(10^{-rt})$, fit to the intact rock experiments of Fig. 1 versus temperature and the inverse of temperature. The right-hand vertical axis gives the decades drop in permeability per year. Error bars, 2σ .

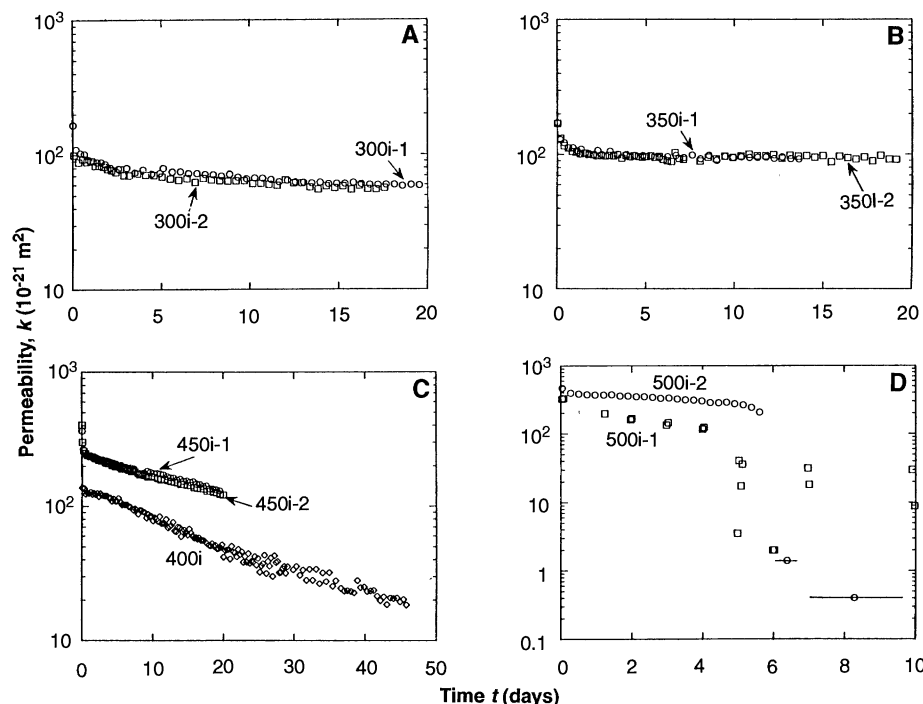


Fig. 1. Permeability of intact Westerly granite. (A) Temperature, 300°C; 300i-1 (circles), 300i-2 (squares). (B) Temperature, 350°C; 350i-1 (circles), 350i-2 (squares). (C) Temperature range, 400° to 450°C; 400i (diamonds), 450i-1 (circles), 450i-2 (squares). (D) Temperature, 500°C; 500i-1 (squares), 500i-2 (circles). The final two data points of experiment 500i-2 measured flow over periods of 0.65 and 3.12 days, respectively, as indicated by the horizontal lines. Essentially no measurable flow was detected during the last 3.12 days of that experiment.

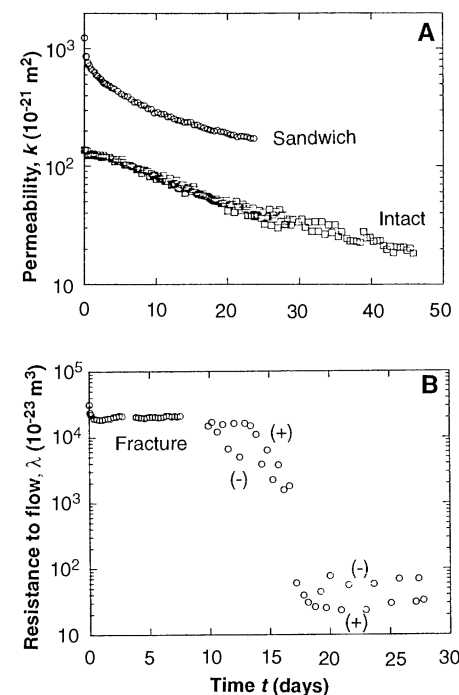


Fig. 3. (A) Comparison of sandwich (400s) and intact granite (400i) experiments at 400°C. (B) Plot of λ versus time for 400°C tensile-fracture experiment (400f). Beginning at about day 10, the flow rate in one direction diverged from that in the other direction, indicated by the (+) and (-) symbols. The direction of faster flow changed from (+) to (-) after day 18. This nonlinear behavior remains unexplained at present. Gaps in the data at day 3 and days 8 to 9 correspond to times when one pore-pressure pump was not operating.

tals were redeposited at other positions along the fracture. These features suggest the operation of solution-transfer processes that redistribute the minerals in the rock, such that asperities are chemically removed while pores and fractures are filled (2, 15). The plagioclase ($Ab_{80}An_{20}$) that dissolved took part in metamorphic reactions. The sodic component of the plagioclase precipitated as albite ($Ab_{96}An_4Or_3$) (Fig. 4), whereas the calcic component combined with other elements to form phases such as a possible actinolitic amphibole.

The changing rate of permeability decrease for the gouge-bearing sample (Fig. 3A) can be explained in terms of the solubilities of some of the gouge materials. Grinding minerals such as quartz to a fine powder creates surface layers of disordered or amorphous material (16) with higher solubilities than that of the undamaged mineral (17). Dissolution of these materials temporarily raises solution concentrations above equilibrium values. In addition, as reviewed by Iler (18), the equilibrium solubility of convex grains of quartz increases markedly with decreasing radius below about 5 nm. The smallest grains therefore dissolve preferentially, and the excess silica in solution is redeposited elsewhere in the sample. The disordered and ultra-fine materials may have been removed from the sample in the first few days of the experiment, leading to the higher initial rates of permeability decrease. Thereafter, the rate declined to the level of intact rock. The high solubility and preferential loss of fines

provide an appealing mechanism for seal formation in active fault zones. Each earthquake shears the fault gouge, producing a fresh zone of ultra-fine particles that quickly dissolve. Subsequent time-dependent compaction expels the supersaturated fluid, which clogs pores and fractures in the surrounding rock (4, 19, 20).

The right-hand vertical axis in Fig. 2 shows the values of τ from Eq. 1 in units of years⁻¹. If the steady exponential decay of permeability in Fig. 1 can be extrapolated, permeability at 400° to 500°C could be reduced by several orders of magnitude in 1 year. The predicted 500°C reductions do not even include the rapid permeability drops at the ends of those experiments (Fig. 1D). These higher temperature results suggest that a well-connected crack network may be impossible to maintain for any appreciable length of time in deeply buried granitic rock, at least in stable cratonic areas. Such a suggestion is consistent with the conclusion derived from geochemical studies that pore waters in the crystalline basement rocks of the Canadian shield are confined to hydrologically isolated pockets (21). At the low-temperature end of Fig. 2, permeability is predicted to decrease by roughly three orders of magnitude within a single year at 300°C, but the yearly decrease at 350°C would be at most about one order of magnitude and possibly substantially less.

The formation of impermeable mineral seals has been invoked at various depths in and around faults. To play an effective role in the earthquake cycle, a seal must be created in less time than the earthquake recurrence interval of a given fault or fault segment, because the seal is likely destroyed by the fracturing and crushing that accompany an earthquake. Our higher temperature results are consistent with the rapid development of impermeable barriers at the base of the seismogenic zone, in accordance with the fault-valve model of Sibson and his colleagues (22). Our lower temperature data provide less conclusive support for models requiring seals at shallower depths in fault zones such as the San Andreas (4, 19, 20), where earthquake recurrence times of 50 to 300 years have been proposed (23). The permeability reduction rates of the experiments at 300°C support the possibility that such seals can develop within the time constraints, but the data at 350°C suggest considerably slower sealing rates. These conflicting results may preclude extrapolation of our data to the lower temperatures of interest for the San Andreas fault, particularly because the mineral reactions should be different. Because of this uncertainty, long-term permeability experiments at lower temperatures are required to obtain an accurate

picture of sealing rates at shallow depths in fault zones. Our results do suggest, however, that the generation of fault gouge should enhance the initial sealing rates at any depth within a fault. In addition, the relatively high permeability of fractures may also be readily reduced by mineral deposition.

REFERENCES AND NOTES

1. R. H. Sibson, in *Earthquake Prediction: An International Review*, D. W. Simpson and A. G. Richards, Eds. (American Geophysical Union, Washington, DC, 1981), pp. 593–603.
2. R. J. Knipe, in *Structural and Tectonic Modelling and Its Application to Petroleum Geology*, R. M. Larsen, H. Brekkem, B. T. Larsen, E. Talleraas, Eds. (Elsevier, Amsterdam, 1992), pp. 325–342.
3. F. M. Chester, J. P. Evans, R. L. Biegel, *J. Geophys. Res.* **98**, 771 (1993).
4. J. Byerlee, *Geology* **21**, 303 (1993).
5. The thermocouple and midpoint of the granite cylinder are positioned at the temperature maximum in the furnace. Temperature decreases by 2% between the middle and ends of the granite sample.
6. During experiment 500i-1, flow in each direction was measured once a day for 1 hour. In the other experiments, flow was reversed by means of a computer command file at intervals of 2×10^4 or 4×10^4 s. The capacity of the smaller pore-pressure pump is 0.28 cm³, and in most cases this entire fluid volume moved through the sample before the direction of flow was reversed. Thus, periods of flow alternated with periods without flow during the experiments. The same small volume of fluid was continually pushed back and forth through the sample. Thus, although the starting fluid in these experiments is deionized water, it should quickly become charged with dissolved material. The more rapid drops in permeability over the first 1 to 2 days of the experiments may reflect a combination of thermal and fluid equilibration processes. Additional information about the experimental assembly and results is provided by D. E. Moore, D. A. Lockner, R. Summers, L. Liu, and J. D. Byerlee (in preparation).
7. Our earlier permeability experiments at elevated temperature [R. Summers, K. Winkler, J. Byerlee, *J. Geophys. Res.* **83**, 339 (1978); C. Morrow, D. Lockner, D. Moore, J. Byerlee, *ibid.* **86**, 3002 (1981); D. E. Moore, C. A. Morrow, J. D. Byerlee, *Geochim. Cosmochim. Acta* **47**, 445 (1983)] involved large gradients in either temperature or fluid pressure, resulting in strong driving forces for mineral precipitation. The current experiments, however, are at nearly uniform pressure and temperature conditions. Our petrographic investigations to date yield no evidence that the pressure and temperature gradients across the samples have led to localization of mineral deposition.
8. Crushed Westerly granite was sieved, and the fraction less than 90 μ m in size was ground in a ball mill to produce a rock flour.
9. Darcy's law is expressed as $k = \mu(q/A)(\Delta l/\Delta P)$, where k is permeability, μ is dynamic viscosity, q is volumetric flow rate, A is cross-sectional area, Δl is sample length, and ΔP is pressure drop. Permeability has units of square meters (alternatively, 1 darcy = 9.87×10^{-13} m²). Flow rate was measured at room temperature. The flow rate in a sample at temperature T was calculated as follows: $q_T = q_{25^\circ\text{C}}(v_T/v_{25^\circ\text{C}})$, where v is the specific volume of the pore water. We estimate that the accuracy of the calculated permeability is within $\pm 5\%$, but the error increases for $k < 1 \times 10^{-21}$ m² (Table 1), which is at the lower measuring limits of the experimental apparatus. Initially, flow through the fractured sample was concentrated in the break rather than distributed through the cylinder. In this case, $A = wd$, where w is fracture width (equal to cylinder diameter) and d is separation between the fracture walls. Because d is not known, it is combined with k to produce a new parameter, λ , where $\lambda = \mu(q/w)(\Delta l/\Delta P)$.

Table 2. Summary of 400°C tensile-fracture experiment (400f). The final heated value is the average of the last two measurements. The final value calculated as k is 34.3×10^{-21} m².

	ΔP (MPa)	q (10^{-6} cm ³ /s)	λ (10^{-23} m ³)
25°C	0.83	171	21600
Heated (initial)	0.08	171	31200
Heated (final)	2.00	6.9	51.4

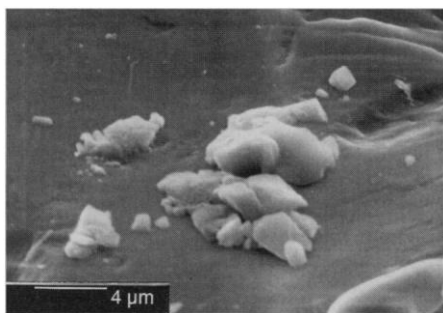


Fig. 4. Secondary-electron SEM image of albite crystals deposited on quartz on the fracture surface of sample 400f.

- Both k and λ relate flow in a crack to the pore-pressure gradient, but λ has units of cubic instead of square meters and is not strictly a crack permeability.
10. W. F. Brace, J. B. Walsh, W. T. Frangos, *J. Geophys. Res.* **73**, 2225 (1968).
 11. J. T. Fredrich and T.-f. Wong, *ibid.* **91**, 12743 (1986).
 12. H. C. Heard and L. Page, *ibid.* **87**, 9340 (1982).
 13. C. H. Scholz, A. Léger, S. L. Karner, unpublished results.
 14. In the equation, c and r are constants. The units are those of the axes in Fig. 1: k and c are in units of 10^{-21} m^2 , t has units of days, and r has units of $days^{-1}$.

15. S. F. Cox, M. A. Etheridge, V. J. Wall, *Ore Geol. Rev.* **2**, 65 (1986).
16. M. S. Paterson and K. Wheatley, *J. Appl. Chem.* **9**, 231 (1959).
17. G. W. Morey, R. O. Fournier, J. J. Rowe, *Geochim. Cosmochim. Acta* **26**, 1029 (1962); R. S. Beckwith and R. Reeve, *ibid.* **33**, 745 (1969).
18. R. K. Iler, *The Chemistry of Silica* (Wiley, New York, 1979).
19. M. L. Blanpied, D. A. Lockner, J. D. Byerlee, *Nature* **358**, 574 (1992).
20. N. H. Sleep and M. L. Blanpied, *ibid.* **359**, 687 (1992).

21. S. K. Frape, P. Fritz, R. H. McNutt, *Geochim. Cosmochim. Acta* **48**, 1617 (1984).
22. R. H. Sibson, F. Robert, K. H. Poulsen, *Geology* **16**, 551 (1988); R. H. Sibson, in *Deformation Mechanisms, Rheology and Tectonics*, R. J. Knipe and E. H. Rutter, Eds. (Geological Society, London, 1992), pp. 15–28.
23. K. Sieh, M. Stuiver, D. Brillinger, *J. Geophys. Res.* **94**, 603 (1989).
24. We thank R. Fournier and C. Williams for comments on an early draft of the manuscript.

2 May 1994; accepted 21 July 1994

Grain Size–Dependent Alteration and the Magnetization of Oceanic Basalts

Dennis V. Kent* and Jeff Gee

Unblocking temperatures of natural remanent magnetization were found to extend well above the dominant Curie points in samples of oceanic basalts from the axis of the East Pacific Rise. This phenomenon is attributed to the natural presence in the basalts of three related magnetic phases: an abundant fine-grained and preferentially oxidized titanomagnetite that carries most of the natural remanent magnetism, a few coarser and less oxidized grains of titanomagnetite that account for most of the high-field magnetic properties, and a small contribution to both the natural remanent magnetism and high-field magnetic properties from magnetite that may be due to the disproportionation of the oxidized titanomagnetite under sea-floor conditions. This model is consistent with evidence from the Central Anomaly magnetic high that the original magnetization acquired by oceanic basalts upon cooling is rapidly altered and accounts for the lack of sensitivity of bulk rock magnetic parameters to the degree of alteration of the remanence carrier in oceanic basalts.

The intensely magnetized oceanic extrusive layer, which consists principally of several hundred meters of sheet flows and pillow basalts, is a major source of sea-floor spreading magnetic anomalies (1). As oceanic crust ages, the basalts are altered and their magnetization becomes substantially reduced, even though a record of the geomagnetic field is retained. A hallmark of the alteration process that is most probably responsible for the reduction in magnetization is a progressive increase in Curie temperature as the original titanomagnetite (TM60) carrier of the natural remanent magnetization (NRM) becomes increasingly oxidized to a cation-deficient titanomaghemite (2). A time constant of 500,000 years has long been assumed for this process, on the basis of analysis of dredged basalts and deep-tow magnetics from the slow-spreading Mid-Atlantic Ridge (MAR) (3–5). To explain the Central Anomaly magnetic high over the fast-spreading East Pacific Rise (EPR), the time constant of magnetization decrease must be only ~20,000 years, more than an order of magnitude faster (6). However, the large variation in NRM intensity found in dredged

basalts from near the axis of the EPR (6) or, for that matter, the MAR (3, 4) was not closely accompanied by a systematic variation in the Curie temperatures of the samples.

A more paradoxical result of some early paleomagnetic studies of dredged basalts from the MAR was that the maximum unblocking temperatures of NRM invariably extended 50° to 100°C above the dominant Curie temperature. The systematic elevation of NRM unblocking temperatures was regarded by Irving (3) as a laboratory artifact and was attributed to the formation during thermal demagnetization of a new higher unblocking temperature phase that inherited its magnetization direction from the parent material. This interpretation was very influential in subsequent rock magnetic studies of oceanic basalts, and thermal demagnetization, a key technique in characterizing remanence in most other rocks, has seldom been used since. In this report, we test the importance of the Irving hypothesis by heating and cooling samples of oceanic basalts under a variety of conditions in the laboratory.

The young basalt samples from the EPR that we studied show a similar systematic discrepancy between unblocking temperature spectrum of NRM and Curie temperature. For example, even after

thermal demagnetization of a sample at 200°C, well above the estimated Curie temperature of 150°C, about 50% of the initial NRM remained (Fig. 1A). The NRM nevertheless had a similar direction over the entire unblocking temperature range (Fig. 1B). The NRM of the EPR ridge axis basalts is thus characterized by significant unblocking of NRM occurring even above 300°C, consistent with an oxidized TM60 as the carrier. Yet, the high-field temperature experiments would suggest that a relatively unoxidized TM60 is the principal magnetic mineral, even though there is little unblocking of NRM by the dominant Curie point.

We initially tried to reproduce the Irving effect in a series of prolonged heating experiments at temperatures of 100° to 300°C in zero field (Fig. 2). The remanence after even 100 hours of heating was not appreciably different from the remanence after the 1 hour of heating typically used in thermal demagnetization. Even when the susceptibility markedly increased over prolonged heating at 300°C, which may have resulted from the inversion of some oxidized TM60 in the sample, the remanence direction and unblocking temperature distribution above 300°C were still essentially unaffected.

We next gave the samples a thermoremanent magnetization (TRM) at a high angle to the NRM direction by cooling them in a 0.03-mT field from 200°C; this temperature is above the dominant Curie point of 150°C but below the unblocking temperatures of ~50% of the NRM. The resulting magnetization was then progressively demagnetized in 25°C steps from 50°C to 600°C (Fig. 3). If the Irving effect were operative, the entire remanence including any unblocking temperature components above the Curie point should have been aligned along the laboratory-induced thermoremanence direction. Instead, the laboratory-induced thermoremanence was effectively demagnetized by 200° to 225°C, and with further thermal demagnetization we recovered the appropriate fraction of the original NRM vector.

The fine-grained EPR basalts showed little evidence of oxidation during these

Lamont-Doherty Earth Observatory of Columbia University, Palisades, NY 10964, USA.

*To whom correspondence should be addressed.